Published in final edited form as:
J Struct Biol. 2007 October ; 160(1): 103–113.

A Freeze Substitution Fixation-Based Gold Enlarging Technique for EM Studies of Endocytosed Nanogold-Labeled Molecules

Wanzhong He[1,4], **Christine Kivork**[1], **Suman Machinani**[1,5], **Mary K. Morphew**[2], **Anna M. Gail**[1,6], **Devin B. Tesar**[1], **Noreen E. Tiangco**[1], **J. Richard McIntosh**[2], and **Pamela J. Bjorkman**[1,3,**]

1*Division of Biology 114-96, California Institute of Technology, 1200 East California Blvd. Pasadena, CA 91125*

2*Boulder Laboratory for 3D Electron Microscopy of Cells, Department of Molecular, Cellular and Developmental Biology, University of Colorado, Boulder, CO 80309*

3*Howard Hughes Medical Institute, California Institute of Technology, 1200 East California Blvd. Pasadena, CA 91125*

Abstract

We have developed methods to locate individual ligands that can be used for electron microscopy studies of dynamic events during endocytosis and subsequent intracellular trafficking. The methods are based on enlargement of 1.4 nm Nanogold attached to an endocytosed ligand. Nanogold, a small label that does not induce misdirection of ligand-receptor complexes, is ideal for labeling ligands endocytosed by live cells, but is too small to be routinely located in cells by electron microscopy. Traditional pre-embedding enhancement protocols to enlarge Nanogold are not compatible with high pressure freezing/freeze substitution fixation (HPF/FSF), the most accurate method to preserve ultrastructure and dynamic events during trafficking. We have developed an improved enhancement procedure for chemically-fixed samples that reduced autonucleation, and a new pre-embedding gold-enlarging technique for HPF/FSF samples that preserved contrast and ultrastructure and can be used for high-resolution tomography. We evaluated our methods using labeled Fc as a ligand for the neonatal Fc receptor. Attachment of Nanogold to Fc did not interfere with receptor binding or uptake, and gold-labeled Fc could be specifically enlarged to allow identification in 2D projections and in tomograms. These methods should be broadly applicable to many endocytosis and transcytosis studies.

**To whom correspondence should be addressed: Tel.: 626-395-8350; Fax: 626-792-3683; E-mail: bjorkman@caltech.edu.
4Present address: Department of Biological Sciences, National University of Singapore, 14 Science Drive 4, Singapore 117543
5Present address: Student Affairs, David Geffen School of Medicine, Los Angeles, CA 90095-1722
6Present address: Molecular Metabolic Control A170, German Cancer Research Center Heidelberg, 69120 Heidelberg, Germany

AUTHOR CONTRIBUTIONS

W.H. designed and implemented the HPF/FSF and chemical fixation gold enlarging methods, administered Au-Fc to rats, prepared tissue samples and performed the corresponding EM experiments. M.K.M. and J.R.M. developed the original concepts for FSF-based silver enhancement. C.K., S.M., A.M.G., D.B.T. and N.E.T. prepared Au-Fc conjugates. D.B.T. and N.E.T. did the confocal microscopy in FcRn-MDCK cells. M.K.M. and P.J.B. did the EM studies in MDCK cells at the Boulder Laboratory for 3D EM of Cells. P.J.B. supervised and planned the project. P.J.B., W.H. and J.R.M. jointly wrote the manuscript.

Keywords

Electron Microscopy; Endocytosis; Fc receptor; Freeze Substitution Fixation; Gold enhancement; High Pressure Freezing; IgG; Nanogold; Electron tomography; Transcytosis

Introduction

Electron microscopy (EM) of cells often requires the use of labeled proteins to identify particular intracellular compartments. For example, gold-labeled antibodies are used to label compartment-specific antigens by immuno-EM. For thick cells that require sectioning, such studies are usually limited to the visualization of antigen near the top and bottom surfaces of a section (e.g., (Griffiths et al., 1984; Ladinsky et al., 2002)). In studies of systems involving endocytosis, labeled ligands are found in all depths of the cell, thus labeling is not limited to the section surfaces. Recent advances in EM tomography of cells allow cell sections to be investigated in 3D rather than with 2D projections, and methods for sample preparation that quickly immobilize all structures involved in dynamic trafficking events, such as rapid freezing, can generate a snapshot of complex cellular events (McIntosh et al., 2005). With high pressure freezing combined with freeze substitution fixation (HPF/FSF), one can obtain ice crystal-free freezing of cultured cells or small tissue samples (Sartori et al., 1993) and a fixation that preserves many aspects of cell ultrastructure (Kellenberger, 1991). Thus studies of intracellular trafficking of labeled ligands by EM tomography have the potential to accurately reveal the 3D itineraries of endocytosed molecules.

Various labeling methods have or could be used to label ligands for EM studies of endocytosis, including attachment of large, electron-dense labels such as colloidal gold (Harding et al., 1983; Murk et al., 2003), ferritin (Rodewald, 1973), or cadmium selenide quantum dots (Glepmans et al., 2005). Other methods involve attachment of labels that are visualized after photooxidation of diaminobenzidine (DAB) and metal deposition (e.g., peroxidase (Rodewald, 1980) and fluorescent labels for correlative light and electron microcopy (Deerinck et al., 1994; Gaietta et al., 2002)). None of these commonly used labels is well-suited for high resolution studies of dynamic events in intracellular trafficking. For example, colloidal gold binds to its ligand non-specifically and non-covalently, binds multiple proteins at once, and tends to aggregate. Smaller colloidal gold particles (1-3 nm) are especially prone to aggregation, leading to large oligomeric gold-antibody structures (Hainfeld and Powell, 2000). The large diameter of ferritin (~14 nm) and its multimeric nature promote undefined ligand-ferritin stoichiometries and cross-linking, which can interfere with the proper trafficking of a ligand (Slade and Wild, 1971). Quantum dots, although promising for correlated fluorescent and electron microscopic studies (Glepmans et al., 2005), are often large (≥10 nm) and most methods for attaching them to proteins of interest either lead to random attachment or, in the case of streptavidin quantum dots, require biotinylation of the ligand and can cause cross-linking resulting from binding to tetrameric streptavidin. Although the labels visualized after photooxidation and metal deposition are generally smaller than colloidal gold, ferritin or quantum dots, the stain that develops from these tags tends to be diffuse, reducing their resolution. Moreover, they are currently incompatible with HPF/FSF methods of sample preservation.

The ideal tracer for a study of endocytosis by electron tomography is a small compound that binds covalently to a ligand without blocking receptor binding, is non-toxic, and does not alter trafficking after being taken up by live cells through endocytosis. A tag with the potential to satisfy these requirements is 1.4 nm Nanogold, a gold cluster that can be conjugated covalently to macromolecules of interest (Hainfeld and Furuya, 1992). However, Nanogold is too small to see by EM in most cellular samples, so it must be enlarged after it has been internalized and

the cells have been fixed. Methods to enhance Nanogold by deposition of silver or gold atoms on clusters in chemically-fixed samples are available (Danscher, 1981; Hacker et al., 1988; Hainfeld and Furuya, 1995; Scopsi, 1989), but when we applied them to chemically-fixed tissue samples containing an endocytosed 1.4 nm Nanogold-ligand, they resulted in high backgrounds due to auto-nucleation and none of these methods is compatible with HPF/FSF samples. Thus, there is a need for methods for enhancing small gold particles after either HPF/FSF or an optimized chemical fixation and before cells are embedded in plastic for microtomy.

Here we evaluated methods to enlarge 1.4 nm Nanogold clusters bound to IgG Fc, a ligand of the neonatal Fc receptor (FcRn). FcRn displays a binding affinity transition that is strongly pH-dependent, such that FcRn binds ligand at the acidic pH found in the gut and intracellular endosomes (pH $\leq$ 6.5) but not at the pH of blood (pH 7.4). This behavior is critical to FcRn's functions both in transporting maternal IgG across epithelial cell barriers, which provides immunity to offspring, and in rescuing serum IgG from degradation (Ghetie and Ward, 2000). We verified that Fc proteins covalently labeled with 1.4 nm Nanogold (Au-Fc) are appropriate ligands to follow FcRn trafficking inside cells by several tests. First, we demonstrated that Au-Fc retains pH-dependent binding to FcRn, is monodisperse, and is endocytosed normally into FcRn-expressing cells. We then used these tagged ligands to develop pre-embedding gold enlarging techniques that are compatible with chemical fixation or with HPF/FSF of tissue samples. Our chemical fixation enhancement method resulted in reduced autonucleation, and our HPF/FSF method extended a new FSF-based silver enhancement method (Morphew et al., 2007) by using gold enhancement to gradually enlarge Nanogold and render it impervious to osmium compounds used during fixation. The resulting methods produced heavy metal labels that were large enough to be visible in 2D projections and tomograms but small enough to provide a spatial resolution that was about as good as EM tomography itself; thus we could reliably identify individual FcRn ligands inside intracellular vesicles in cells expressing FcRn. These methods should also be applicable to a wide range of EM tomography studies of endocytosis in other systems.

METHODS

Preparation of 1.4 nm gold-labeled Fc (Au-Fc)

The Fc fragment from rat IgG2a was expressed in Chinese hamster ovary cells and purified as described (Martin and Bjorkman, 1999). Conditions to selectively reduce hinge disulfides were obtained by evaluating the results of different reduction protocols using Ellman's Reagent (Pierce Chemicals). 1.0 - 1.5 mg of Fc was reduced with 12-18 mg of mercaptoethylamine hydrochloride in 1 ml of 0.1 M $NaPO_4$ pH 6.0, 5 mM EDTA for 1.5 hours at 37 °C, then passed over a Superdex 75 size exclusion column (Pharmacia) in 20 mM $NaPO_4$ pH 6.5, 150 mM NaCl, 1 mM EDTA.

After concentration, the reduced Fc was labeled with 1.4 nm monomaleimido Nanogold® (Nanoprobes, Inc.), which reacts specifically with reduced sulfhydryls (Hainfeld and Furuya, 1992), following the manufacturer's protocol for labeling IgG. Briefly, ~30 nmol of 1.4 nm monomaleimido Nanogold was suspended in 1 ml deionized water, then immediately incubated with the reduced Fc for 2-4 hours at room temperature. Labeled Fc (Au-Fc) was separated from unlabeled Fc and free Nanogold by passage over the Superdex 75 gel filtration column. Labeled Fc was further purified by passage over an FcRn affinity column at pH 6, followed by elution at pH 8, as described (Huber et al., 1993). The molar concentrations of Nanogold and Fc were determined spectrophotometrically at 420 nm and 280 nm, respectively, using extinction coefficients of 155,000 $M^{-1}cm^{-1}$ for Nanogold and 60,900 $M^{-1}cm^{-1}$for Fc. The A_{280} for Fc was corrected for Nanogold absorption at 280 nm as described in the Nanoprobes protocol.

Au-Fc uptake in neonatal rats

11- to 13-day suckling rats born to Sprague Dawley rats were separated from their mothers for ~3 hours, then fed 3 × 100 μl (at 45-60 min intervals) of Au-Fc (~2 μM) in 20 mM $NaPO_4$, 1.2 mM $CaCl_2$, 0.5 mM $MgCl_2$, 0.25 mM $MgSO_4$, pH 6.0 at 37°C. After 2-3 hours, rats were anesthetized with CO_2, sacrificed, and the small intestine was removed by dissection. From each intestine, a 4 - 5 cm segment of proximal small intestine, starting ~2 cm from the pylorus, and a 4 - 5 cm segment of the distal small intestine (ileum), located ~2 cm from the ileocecal valve, were removed for chemical fixation or high pressure freezing. Within the proximal small intestine, the jejunum can be distinguished from the duodenum by the presence of the characteristic suspensory muscle of the duodenum (the ligament of Treitz).

Gold enhancement of chemically-fixed intestinal samples

Small intestine segments were quickly cut into small pieces, then immediately fixed in 3% glutaraldehyde and 1% formaldehyde (Electron Microscopy Sciences) in 0.1 M sodium phosphate pH 6.0, 2 mM $CaCl_2$, 1 mM $MgCl_2$, 0.5 mM $MgSO_4$ for 30 min at 20°C. Fixation was continued for 3-4 hours at 4°C in the same buffer at pH 7.4, and then segments were rinsed with 0.1 M sodium phosphate pH 7.4 before gold enhancing.

Initially, we used a gold enhancement kit, GoldEnhance-EM 2113 (Nanoprobes, Inc.), to enlarge Nanogold internalized by the cells in intestinal segments, but the solutions and protocol supplied by the manufacturer resulted in rapid enhancement (2-3 minutes) and substantial levels of auto-nucleation. Our modified protocol was as follows: Samples were washed 3 × 5 min with PBS including glycine (20 mM sodium phosphate pH 7.4, 150 mM NaCl, 50 mM glycine) to remove aldehydes, 3 × 5 min with PBS-BSA-Tween (PBS containing 1% BSA and 0.05% Tween 20), and then 3 × 5 min with 5 mM sodium phosphate pH 5.5, 100 mM NaCl (Solution E). For gold enhancement, we placed 1-5 intestinal samples (~1 mm × ~1 mm) in a mixture of the manufacturer's Solutions A and B at a 2:1 ratio (~80 μl of A and ~40 μl of B). After 5 min, we added ~200 μl of Solution E with 20% gum arabic (Sigma-Aldrich) and then ~80 μl of Solution C. After 7-15 minutes of development, samples were transferred to 1-2% sodium thiosulfate to stop the enhancement. Samples were then washed 3 × 5 min with buffer E. This protocol resulted in slower development, reduced background and improved uniformity of enhanced particle size, especially when the enhancement was conducted at 4°C rather than room temperature. In the absence of gum arabic, there were variations in the sizes of enlarged gold particles (Figure 3b, left panel), perhaps resulting from differences in the time it took for the sodium thiosulfate stopping solution to reach different portions of the cell.

Gold-enhanced, chemically-fixed samples were incubated in 1% OsO_4 in 0.1 M sodium phosphate pH 6.1 for 60 min, and then rinsed with distilled H_2O prior to 1 hr staining *en bloc* with 2% uranyl acetate. Samples were dehydrated with progressive lowering of temperature as described (Berryman and Rodewald, 1990; Gounon and Rolland, 1998) in a Leica EM AFS machine (Leica Microsystems).

HPF/FSF of intestinal samples

Intestinal samples were rapidly frozen with a BAL-TEC HPM 010 High Pressure Freezer (Bal-Tec, AG). An intestinal segment was transferred into the 200 μm deep side of a 100μm/200μm specimen carrier that was ~2 mm in diameter (Engineering Office M. Wohlwend GmbH, Switzerland). The specimen chamber was filled with 1-hexadecene (Sigma-Aldrich) and then sandwiched against the flat side of a 300 μm specimen carrier. This sandwiched carrier was placed in the sample holder, then high pressure frozen at 2100 bar and transferred to liquid nitrogen for storage. The time interval between initial cutting of the sample and freezing was 30-40 s.

For conventional FSF of unenhanced samples, the specimen carriers with frozen samples were transferred to 1.5 ml microcentrifuge tubes (Fisher Scientific, U.S.A.) containing a frozen solution of acetone with 1% OsO_4 and 0.1% uranyl acetate under liquid nitrogen. Tubes were placed in a Leica EM AFS machine (Leica Microsystems) at -140°C and gradually warmed to - 90°C in 4 hrs. The temperature was then gradually raised in 6 hr transitions in the Leica AFS system as follows: -90°C for 24-48 hr, -60°C for 24 hr, and -30°C for 18 hr. After slowly warming to 0°C over 2 hours, samples were washed three times in pure acetone and warmed to room temperature.

Silver enhancement/gold-toning/gold enhancement during FSF of HPF samples

The FSF procedure described above was modified to include a preembedding gold-enlarging technique for HPF cells by adapting approaches that involve silver or gold enhancement at room temperature (Danscher, 1981; Hacker et al., 1988; Hainfeld and Furuya, 1995; Scopsi, 1989), gold-toning (Sawada and Esaki, 2000), seed-mediated gold-enlarging (Busbee et al., 2003; Daniel and Astruc, 2004; Gole and Murphy, 2004; Handley, 1989; Jana et al., 2001; Meltzer et al., 2001; Okitsu et al., 2005; Zou et al., 2006) and a FSF-based silver-enhancement procedure (Morphew et al., 2007). To avoid the background that results from spontaneous auto-nucleation, we designed a three-step enlarging protocol in which silver enhancement was used to slightly enlarge the Nanogold, the silver shell was coated by gold toning to make it insoluble in osmium, and the particles were further enlarged to 10 - 16 nm using gold enhancement.

Samples were first added to a 1.2 ml solution of acetone including 0.5% glutaraldehyde and the temperature was raised from -140°C to -60°C as described above for the conventional FSF protocol. Samples were then washed with acetone at -60°C (3 × 4 hr each) to remove unreacted glutaraldehyde. An HQ or LI silver enhancing solution (Nanoprobes, Inc.) was prepared at 4° C according to the manufacturer's instructions. Immediately after preparation, 20 μl of enhancing solution was quickly frozen by injection into liquid nitrogen. A silver enhancing mixture was prepared by adding 50 μl of saturated sodium citrate (0.1g sodium citrate added to 10 ml of acetone at 4°C) and 50 μl of saturated Na_2CO_3 (0.1g Na_2CO_3 added to 10 ml of acetone at 4°C) to 1 ml of saturated $AgNO_3$ (0.1 g $AgNO_3$ added to 10 ml of acetone-methanol solution (98%:2%) in a foil-covered tube) on dry ice, then adding the frozen drop of HQ or LI silver enhancing solution. After mixing in a foil-sealed tube, 1.2 ml of the silver enhancing mixture was added to the intestinal samples at -60°C and incubated for 8 - 12 hours.

After rinsing samples with acetone (3 × 2 hours) at -60°C, gold toning was done by incubating the samples in 1.2 ml of a gold-toning mixture, 0.1% $HAuCl_4 \cdot 3H_2O$ (Sigma-Aldrich) in acetone-methanol (98%:2%), for 8 - 12 hours at -60°C. The gold enhancement procedure used a frozen 20 μl sample of a room temperature gold enhancement reagent, GoldEnhance-EM 2113 (Nanoprobes, Inc.), prepared by freezing 20 μl in liquid nitrogen as described for Silver LI and Silver HQ above. Saturated solutions of L-ascorbic acid (kept in the dark) and K_2CO_3 (Sigma-Aldrich) were prepared by adding 0.1 g of the relevant chemical to 10 ml acetone-methanol solution on ice. A fresh solution of saturated $NaBH_4$ (Sigma-Aldrich) was prepared similarly on dry ice in the dark. The gold-enhancing mixture was prepared by adding the frozen drop of gold enhancement reagent plus 80 μl of the ascorbic acid solution, 50 μl of the K_2CO_3 solution, and 20-50 μl of $NaBH_4$ solution to 1 ml of 0.01-0.1% $HAuCl_4 \cdot 3H_2O$ in acetone-methanol (98%:2%) on dry ice. The gold-enhancing mixture was applied to samples for 24 hours at -60°C. Samples were then rinsed with 1.2 ml acetone at the same temperature (3 × 4 hours), and then 1.2 ml of 1% OsO_4 and 0.1% uranyl acetate in acetone was added to samples, followed by warming to - 30°C. Warming to room temperature was done as described above for unenhanced FSF samples.

Further optimization of the protocol might result in increased reliability and a decrease in the number of steps and/or reagents involved. For example, it might be possible to replace the

above silver enhancement step with the optimized protocol described in (Morphew et al., 2007). However, the current protocol usually resulted in enlargement of 1.4 nm Nanogold while avoiding significant background auto-nucleation. If auto-nucleation did occur, it could usually be prevented by diluting the saturated reducing solution and/or reducing the development time in each of the three steps. To prevent nucleation due to deposition of silver or gold onto metal contaminants, we avoided any external sources of metal particles during the HPF/FSF and gold enlarging steps. Enlarged gold particles resulting from external seed particles were found on rare occasions, but these were larger and more irregular in shape than enhanced 1.4 nm Nanogold. A quantitative analysis of gold particles in >50 tomograms in HPF/FSF/enhanced intestinal cell samples revealed that ≥98% of enlarged gold particles represented Au-Fc bound to FcRn (He et al., 2007).

Embedding and Electron Microscopy

Chemically-fixed or HPF/FSF intestinal samples were infiltrated, embedded, polymerized, sectioned and stained as previously described (He et al., 2003). Selected regions of 70 - 200 nm sections were examined using an FEI T12 G2 Electron Microscope operating at 120 kV, and projection images were recorded on a Gatan 894 2K × 2K CCD camera (Gatan Corporation). Tilt series (±70°, 1.0° angular increments) were digitally recorded at 6500x (pixel size =1.57 nm) and at 700 nm underfocus about two orthogonal axes on the Gatan camera, using the microscope control program SerialEM as described (Mastronarde, 2005). Tomograms were computed for each tilt axis using the enlarged gold particles as markers for alignment, and then aligned to each other and combined using the IMOD software package (Kremer et al., 1996; Mastronarde, 1997).

Additional Methods—Further information on methods and results related to studies in FcRn-expressing MDCK cell is available in **Supplementary Information**.

RESULTS

Au-Fc retained pH-dependent binding to FcRn

To obtain a homogenous preparation of labeled Fc that retained binding to FcRn, we used a monomaleimido-derivatized 1.4 nm gold cluster to label reduced cysteines in the Fc hinge region, which can be selectively reduced without affecting intradomain disulfides (Williamson and Askonas, 1968). The hinge region is distant from the FcRn binding site at the interface between the Fc C_H2 and C_H3 domains (Martin et al., 2001) (Figure 1a), thus increasing the likelihood that the labeled proteins will retain functional FcRn binding.

Our labeling protocol involved two sequential purification steps: first, size exclusion gel filtration to separate labeled Fc (Au-Fc) from unlabeled Fc and free Nanogold, and second, an FcRn affinity column (Huber et al., 1993) to ensure that the Au-Fc retained pH-dependent binding to FcRn. Results from size exclusion columns showed a shift in migration consistent with covalent attachment of Nanogold and no signs of Au-Fc aggregation (Figure 1b). Nanogold/Fc ratios after FcRn affinity chromatography were typically 0.8 - 1.1, suggesting that most or all of the Fc molecules were labeled, consistent with SDS-PAGE analysis (Figure 1c). Intact human IgG, however, demonstrated poor labeling efficiency when subjected to the same labeling protocol (data not shown). Since intact IgG and Fc bind with similar affinities and pH-dependent binding profiles to rat FcRn (Vaughn and Bjorkman, 1997), we used the more efficiently-labeled Au-Fc, rather than Au-IgG, as a ligand for FcRn in subsequent experiments.

We used confocal microscopy to study an MDCK cell line that expresses rat FcRn and had previously been shown to bind, internalize, and bidirectionally transcytose rat IgG and Fc

(Tesar et al., 2006). Our results showed that Au-Fc was bound by and endocytosed normally into these polarized cells by FcRn (Figure 1d and Supplementary Methods). Examination of these cells by EM, however, showed that 1.4 nm Nanogold was too small to be routinely localized in cells with 2D projections or tomograms (Supplementary Figure 1 and Supplementary Information).

Specific enhancement of endocytosed 1.4 nm Au-Fc in chemically-fixed intestinal cells

To facilitate locating 1.4 nm Au-Fc inside cells, we used gold enhancement to deposit gold atoms specifically on the 1.4 nm Nanogold, thereby enlarging the particles to 10-20 nm. These experiments were done using intestinal samples from neonatal rats that had been fed Au-Fc. The concentration of Au-Fc that was fed to neonatal rats was 2-3 μM, approximately equal to the IgG concentration in rat milk, because higher concentrations saturate FcRn, resulting in degradation of excess IgG (Benlounes et al., 1995). In this system for Au-Fc uptake, we had two controls for the specificity of uptake and gold enhancement: first, the presence or absence of ingested Au-Fc, and second, the requirement that enhanced gold particles should appear in physiologically-relevant locations in cells; e.g., in locations corresponding to FcRn expression (apical cell surface, coated vesicles and tubulovesicular compartments) in samples from the proximal small intestine, and inside degradative compartments (e.g., giant lysosomes) in samples from the neonatal distal small intestine (ileum), which does not express FcRn (Rodewald, 1973).

Our original attempts to enhance chemically-fixed tissues resulted in significant background color development, which came from auto-nucleation in both the Au-Fc-fed intestinal sample and the control sample (Figure 2a,c). We therefore modified the enhancement protocol to slow the development time, resulting in specific enhancement such that the control intestinal sample did not show significant color development, and the Au-Fc-fed sample retained color development (Figure 2b). EM images confirmed specific enhancement in that enhanced gold particles were found in giant lysosomes within samples derived from the neonatal ileum of Au-Fc-fed rats but not in neighboring goblet cells of the same sample (Figure 3a). These results are consistent with the function of neonatal ileal cells in fluid phase uptake and degradation, and the secretory, rather than uptake, function of goblet cells (Rodewald, 1973). As another demonstration of specific enhancement, we found enhanced gold particles at the apical cell surface and inside tubular intracellular vesicles in the proximal small intestine (Figure 3b), consistent with FcRn-mediated uptake in this region. In the distal small intestine, the majority of gold particles were in large lysosomes (Figure 3a), consistent with fluid-phase uptake in the distal small intestine, which does not express FcRn (Rodewald, 1973). In both proximal and distal intestinal samples, we did not see enhanced gold particles in organelles such as the mitochondria or the nucleus (data not shown), indicating that the enlarged gold particles corresponded to specifically-enhanced Au-Fc that had been endocytosed into intracellular vesicles.

A new method to enlarge 1.4 nm gold clusters in HPF/FSF samples

Having used chemically-fixed neonatal intestinal samples to confirm that Au-Fc is taken up through fluid phase endocytosis in the distal small intestine and an FcRn-mediated pathway in the proximal small intestine, we next worked out a method to enlarge Au-Fc in HPF/FSF samples. Of critical importance for our efforts was the recent development of a silver enhancement method compatible with FSF, the first demonstration that enlargement of Nanogold is possible in organic solvents at low temperature (Morphew et al., 2007). In this method, Nanogold particles were enlarged to 3-8 nm in tissue samples using a mixture of silver nitrate, hydroquinone, sodium citrate and sucrose in cold acetone. The resulting particles could be seen in tomograms, but were not large enough to be visualized in 2D projections (Morphew et al., 2007). In addition, a general limitation of silver enhancement methods is that osmium

compounds, which improve the preservation of membranes, cannot be added during fixation because they dissolve the layer of added silver (Hainfeld et al., 1999). To address both of these issues, we combined silver enhancement during FSF with gold toning and gold enhancement to increase the size of the enlarged particles and render them impervious to osmium compounds used during fixation.

Silver enhanced/gold-toned/gold enhanced HPF/FSF duodenal samples showed that the Nanogold was enlarged to 10-16 nm and was easily visible in both projection images (Figure 4) and tomograms (Figure 5). The ability to directly visualize enlarged gold particles in projection images allows one to choose a region containing Au-Fc for subsequent tomography, and a tilt series can be recorded at a magnification (e.g., 6500x) that enables the reconstruction of a reasonably large portion of the cell. Our enhancement protocol was compatible with the use of OsO_4 and uranyl acetate, thereby preserving contrast and details of the ultrastructure. Both projections (Figure 4) and digital slices from tomograms (Figure 5) showed high contrast and smooth membranes in both vesicles and cells, thus the gold enlarging procedure did not reduce the high resolution possible with HPF/FSF. The enlarged gold particles were in locations suggesting they represented enhanced 1.4 nm Nanogold attached to Fc that was bound to FcRn: near the inner membrane leaflets of tubular vesicles (Figure 4a and 5) and multivesicular bodies (Figure 4b), and in the extracellular space near the basolateral surface (Figure 4c, 5d). Notably, the majority of enhanced Au-Fc particles in duodenal samples were found within a 6-7 nm distance from a membrane, implying attachment to FcRn, which has an ~5 nm ectodomain (Burmeister et al., 1994). In the ileum, we again saw enhanced gold particles inside degradative vesicles (Figure 4d), consistent with fluid phase uptake in this region of the neonatal intestine. The specificity of gold enlargement is demonstrated by comparing Figures 4a-d with Figure 4e, an example of non-specific enhancement in an HPF/FSF sample that was reduced too harshly and/or developed for too long. Such problems can usually be avoided by diluting the saturated reducing chemicals and/or reducing the developing times for the three steps in the enhancement procedure.

DISCUSSION

Here we have demonstrated that a 1.4 nm gold-labeled Fc is a reliable tag for EM studies of receptor-mediated endocytosis and transport by FcRn. A monomaleimido-derivatized Nanogold was attached to Fc without affecting FcRn binding or uptake into cells. Although the small size of 1.4 nm Nanogold makes it ideal for preserving the proper binding and function of a labeled ligand, these clusters were not large enough to be located directly in EM projection images and in most tomograms derived from stained cell sections. We therefore adapted autometallography and nanoparticle seeding techniques that are used to enlarge 1.4 nm Nanogold clusters by selectively depositing silver and/or gold atoms onto their surfaces (Busbee et al., 2003; Daniel and Astruc, 2004; Gole and Murphy, 2004; Hainfeld and Furuya, 1995; Hainfeld et al., 1999; Jana et al., 2001; Meltzer et al., 2001; Okitsu et al., 2005; 1989; Zou et al., 2006).

We initially concentrated on gold enhancement of neonatal rat intestinal samples that had been chemically fixed in order to quickly screen for specific Au-Fc uptake. Based on previous studies of IgG transport in the neonatal rat intestine (Rodewald, 1973), we expected to see FcRn-mediated uptake in the proximal small intestine and fluid-phase uptake in the distal small intestine of a rat that has been fed Au-Fc. However, our first attempts using published gold-enhancing protocols resulted in non-specific background deposition in both types of sample. The modifications described here reduced non-specific background in gold-enhanced chemically-fixed samples, and showed images confirming specific enhancement in the different regions of the intestine. The reduction of autonucleation and improved control over

development with our method should benefit other pre-embedding enhancement efforts involving chemically-fixed tissue samples.

Having demonstrated that Au-Fc is a reliable marker for receptor-mediated and fluid phase endocytosis following chemically fixation, we next undertook to enlarge Nanogold in tissue samples prepared by HPF/FSF methods, which is preferable to chemical fixation for studies of dynamic events during intracellular trafficking (McIntosh et al., 2005). Expanding upon a previously-described FSF-based method involving silver enhancement (Morphew et al., 2007), we developed a new gold-enlarging method for HPF/FSF samples that combines gold toning and gold enhancement, following an initial silver enhancement step. Including gold enhancement in our method offers two potential advances: First, unlike silver, gold is not dissolved by osmium tetroxide (Hainfeld et al., 1999), a commonly-used fixative in EM applications that results in optimal contrast of membrane structures. Second, by using gold enhancement following silver enhancement, we could enlarge the Nanogold clusters to 10-16 nm, which allows for direct visualization of particles in 2D projections prior to the selection of a region for tomography. By contrast, it was not possible to visualize enhanced particles in 2D projections using silver enhancement alone because the particles were enlarged to ≤8 nm (Morphew et al., 2007). In principle, the gold toning and gold enhancement steps could be used without a prior silver enhancement step in a HPF/FSF gold enlarging procedure. However, we obtained optimal results (less auto-nucleation and a greater uniformity in particle size) by combining the silver enhancement step with gold toning and gold enhancement. When auto-nucleation did occur, we could distinguish auto-nucleated particles from enhanced 1.4 nm Nanogold in EM images because the former were smaller and randomly distributed as compared with the latter.

We conclude that the combination of thiol-specific Nanogold labeling to obtain a minimally-perturbed ligand with subsequent gold-enlargement allows the use of high-resolution electron tomography to accurately trace receptor-ligand complexes during endocytosis and intracellular trafficking.

Supplementary Material

Refer to Web version on PubMed Central for supplementary material.

ACKNOWLEDGEMENTS

We thank D.N. Mastronarde for advice on setting up SerialEM on the Caltech microscopes, E.T. O'Toole (University of Colorado) for help with IMOD, R.D. Powell (Nanoprobes, Inc.) for advice on gold enhancement, C.J. Ackerson and R.D. Kornberg (Stanford University) for preparing MPC gold bound to Fc for testing, and G.J. Jensen and W.F. Tivol (Caltech) for the use of the T12 microscope. This work was supported by the National Institutes of Health (2 R37 AI041239-06A1 to P.J.B.; RR000592 to J.R.M.) and gifts to Caltech to support electron microscopy from the Gordon and Betty Moore Foundation and the Agouron Institute.

References

Benlounes N, Chedid R, Thuillier F, Desjeux JF, Rousselet F, Heyman M. Intestinal transport and processing of immunoglobulin G in the neonatal and adult rat. Biol Neonate 1995;67:254–263. [PubMed: 7647150]

Berryman MA, Rodewald RD. An enhanced method for post-embedding immunocytochemical staining which preserves cell membranes. J Histochem Cytochem 1990;38:159–170. [PubMed: 1688894]

Burmeister WP, Gastinel LN, Simister NE, Blum ML, Bjorkman PJ. Crystal structure at 2.2 Å resolution of the MHC-related neonatal Fc receptor. Nature 1994;372:336–343. [PubMed: 7969491]

Busbee BD, Obare SO, Murphy CJ. An improved synthesis of high-aspect-ratio gold nanorods. Adv Mater 2003;15:414–416.

Daniel MC, Astruc D. Gold nanoparticles: Assembly, supramolecular chemistry, quantum-size-related properties, and applications toward biology, catalysis, and nanotechnology. Chemical Reviews 2004;104:293–346. [PubMed: 14719978]

Danscher G. Histochemical demonstration of heavy metals. A revised version of the sulphide silver method suitable for both light and electronmicroscopy. Histochemistry 1981;71:1–16. [PubMed: 6785259]

Deerinck TJ, Martone ME, Lev-Ram V, Green DPL, Tsien RY, Spector DL, Huang S, Ellisman MH. Fluorescence photooxidation with eosin: A method for high resolution immunolocalization and in situ hybridization detection for light and electron microscopy. J Cell Biol 1994;126:901–910. [PubMed: 7519623]

Gaietta G, Deerinck TJ, Adams SR, Bouwer J, Tour O, Laird DW, Sosinsky GE, Tsien RY, Ellisman MH. Multicolor and electron microscopic imaging of connexin trafficking. Science 2002;296:503–507. [PubMed: 11964472]

Ghetie V, Ward ES. Multiple roles for the major histocompatibility complex class I-related FcRn. Annu Rev Immunol 2000;18:739–766. [PubMed: 10837074]

Glepmans BNG, Deerinck TJ, Smarr BL, Jones YZ, Ellisman MH. Correlated light and electron microscopic imaging of multiple endogenous proteins using Quantum dots. Nature Methods 2005;2:743–749. [PubMed: 16179920]

Gole A, Murphy CJ. Seed-mediated synthesis of gold nanorods: Role of the size and nature of the seed. Chemistry of Materials 2004;16:3633–3640.

Gounon P, Rolland JP. Modification of Unicryl composition for rapid polymerization at low temperature without alteration of immunocytochemical sensitivity. Micron 1998;29:293–296. [PubMed: 9744087]

Griffiths G, McDowall A, Back R, Dubochet J. On the preparation of cryosections for immunocytochemistry. J Ultrastruct Res 1984;89:65–78. [PubMed: 6544882]

Hacker GW, Grimelius L, Danscher G, Bernatzky G, Muss W, Adam H, Thurner J. Silver acetate autometallography -- An alternative enhancement technique for immunogold-silver staining (IGSS) and silver amplification of gold, silver, mercury and zinc in tissues. J Histotechnol 1988;11:213–221.

Hainfeld JF, Furuya FR. A 1.4-nm gold cluster covalently attached to antibodies improves immunolabeling. J Histochem Cytochem 1992;40:177–184. [PubMed: 1552162]

Hainfeld, JF.; Furuya, FR. Silver-enhancement of Nanogold and undecagold, In Immunogold-silver staining: Principles, methods and applications. Hayat, MA., editor. CRC Press; Boca Raton, FL: 1995. p. 71-96.

Hainfeld JF, Powell RD. New frontiers in gold labeling. J Histochem & Cytochem 2000;48:471–480. [PubMed: 10727288]

Hainfeld, JF.; Powell, RD.; Stein, JK.; Hacker, GW.; Hauser-Kronberger, C.; Cheung, ALM.; Schofer, C. In: Bailey, GW.; Jerome, WG.; McKernan, S.; Mansfield, JF.; Price, RL., editors. Gold-based autometallography; Proc. 57th Ann. Mtg, Micros. Soc. Amer.; New York, NY: Springer-Verlag; 1999. p. 486-487.

Handley, DA. Methods for Synthesis of Colloidal Gold, In Colloidal Gold: Principles, Methods, and Applications. Hayat, MA., editor. Academic Press; San Diego: 1989. p. 13-30.

Harding C, Heuser J, Stahl P. Receptor-mediated endocytosis of transferrin and recycling of the transferrin receptor in rat reticulocytes. J Cell Biol 1983;97:329–339. [PubMed: 6309857]

He W, Cowin P, Stokes DL. Untangling desmosomal knots with electron tomography. Science 2003;302:109–113. [PubMed: 14526082]

HeWJensenGJMcIntoshJRBjorkmanPJThree-dimensional itinerary of FcRn-mediated antibody transport across epithelial cells revealed by electron tomography. ms in preparation 2007

Huber AH, Kelley RF, Gastinel LN, Bjorkman PJ. Crystallization and Stoichiometry of Binding of a Complex between a Rat Intestinal Fc Receptor and Fc. J Mol Biol 1993;230:1077–1083. [PubMed: 8478919]

Jana NR, Gearheart L, Murphy CJ. Evidence for Seed-Mediated Nucleation in the Chemical Reduction of Gold Salts to Gold Nanoparticles. Chem Mater 2001;13:2313–2322.

Kellenberger E. The potential of cryofixation and freeze substitution: observations and theoretical considerations. J Microsc 1991;161:183–203. [PubMed: 1903815]

Kremer JR, Mastronarde DN, McIntosh JR. Computer visualization of three-dimensional data using IMOD. J Struct Biol 1996;116:71–76. [PubMed: 8742726]

Ladinsky MS, Wu CC, McIntosh S, McIntosh JR, Howell KE. Structure of the Golgi and distribution of reporter molecules at 20 degrees C reveals the complexity of the exit compartments. Mol Biol Cell 2002;13:2810–2825. [PubMed: 12181348]

Martin WL, Bjorkman PJ. Characterization of the 2:1 complex between the class I MHC-related Fc receptor and its Fc ligand in solution. Biochem 1999;38:12639–12647. [PubMed: 10504233]

Martin WL, West AP, Gan L, Bjorkman PJ. Crystal structure at 2.8 Å of an FcRn/heterodimeric Fc complex: Mechanism of pH dependent binding. Molecular Cell 2001;7:867–877. [PubMed: 11336709]

Mastronarde DN. Dual-axis tomography: an approach with alignment methods that preserve resolution. J Struct Biol 1997;120:343–352. [PubMed: 9441937]

Mastronarde DN. Automated electron microscope tomography using robust prediction of specimen movements. J Struct Biol 2005;152:36–51. [PubMed: 16182563]

McIntosh JR, Nicastro D, Mastronarde DN. New views of cells in 3D: an introduction to electron tomography. Trends Cell Biol 2005;15:43–51. [PubMed: 15653077]

Meltzer S, Resch R, Koel BE, Thompson ME, Madhukar A, Requicha AAG, Will P. Fabrication of nanostructures by hydroxylamine seeding of gold nanoparticle templates. Langmuir 2001;17:1713–1718.

MorphewMHeWBjorkmanPJMcIntoshJRSilver enhancement of nanogold particles during freeze substitution fixation for electron microscopy. J Microscopy in press 2007

Murk JLAN, Humbel BM, Ziese U, Griffith JM, Posthuma G, Slot JW, Koster AJ, Verkleij AJ, Geuze HJ. Endosomal compartmentalization in three dimensions: Implications for membrane fusion. Proc Natl Acad Sci USA 2003;100:13332–13337. [PubMed: 14597718]

Okitsu K, Teo BM, Ashokkumar M, Grieser F. Controlled growth of sonochemically synthesized gold seed particles in aqueous solutions containing surfactants. Australian Journal of Chemistry 2005;58:667–670.

Rodewald R. Intestinal transport of antibodies in the newborn rat. J Cell Biol 1973;58:189–211. [PubMed: 4726306]

Rodewald R. Distribution of immunoglobulin G receptors in the small intestine of the young rat. J Cell Biol 1980;85:18–32. [PubMed: 7364873]

Sartori N, Richter K, Dubochet J. Vitrification depth can be increased more than 10-fold by high-pressure freezing. J Microscopy 1993;172:55–61.

Sawada H, Esaki M. A practical technique to postfix nanogold-immunolabeled specimens with osmium and to embed them in Epon for electron microscopy. J Histochem Cytochem 2000;48:493–498. [PubMed: 10727291]

Scopsi, L. Silver-enhanced Colloidal Gold Method, In Colloidal Gold: Principles, Methods, and Applications. Hayat, MA., editor. Academic Press; San Diego: 1989. p. 252-288.

Slade BS, Wild AE. Transmission of human gamma-globulin to rabbit foetus and its inhibition by conjugation with ferritin. Immunology 1971;20:217–223. [PubMed: 4100988]

Tesar DB, Tiangco NE, Bjorkman PJ. Ligand valency affects FcRn-mediated transcytosis, recycling, and intracellular trafficking. Traffic 2006;7:1–16.

Vaughn DE, Bjorkman PJ. High-affinity binding of the neonatal Fc receptor to its IgG ligand requires receptor immobilization. Biochemistry 1997;36:9374–9380. [PubMed: 9235980]

Williamson AR, Askonas BA. Differential reduction of interchain disulphide bonds of mouse immunoglobulin G. Biochem J 1968;107:823–828. [PubMed: 16742608]

Zou X, Ying E, Dong S. Seed-mediated synthesis of branched gold nanoparticles with the assistance of citrate and their surface-enhanced Raman scattering properties. Nanotechnology 2006;17:4758–4764.

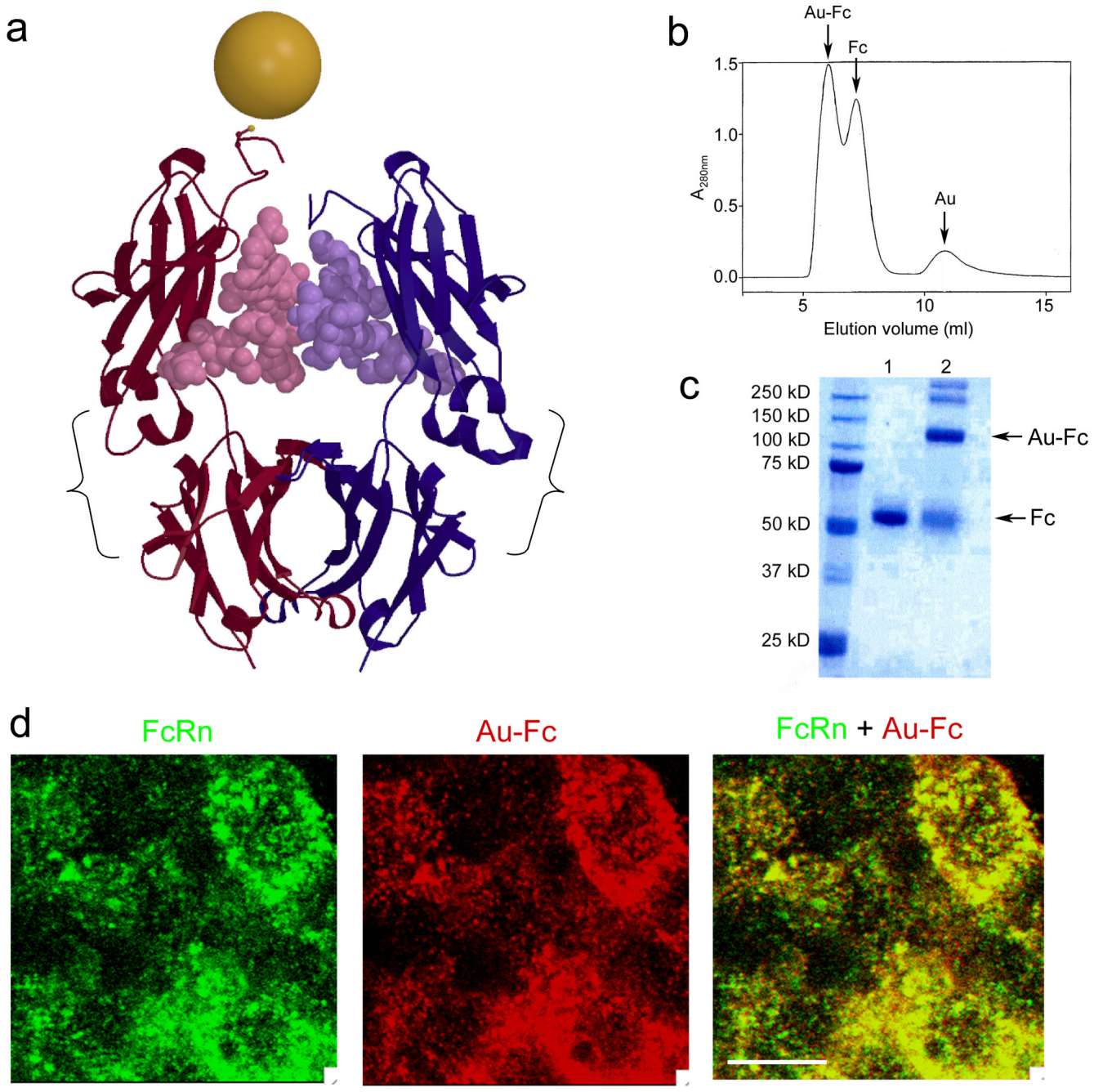

Figure 1.

Preparation of Au-Fc. (a) Ribbon diagram of the structure of Fc (pdb code 1I1c) with a gold sphere (drawn to scale) representing a 1.4 nm monomaleimido Nanogold covalently attached to a reduced cysteine in the Fc hinge region. One Nanogold is depicted, based on the calculated Nanogold/Fc ratios obtained in most labeling reactions (0.8 - 1.1). The Nanogold cluster bound in a region that is distant from the FcRn binding site (indicated on each Fc chain with a bracket). (b) S75 Superdex gel filtration profile following incubation of reduced Fc with 1.4 nm Nanogold. (c) 10% SDS-PAGE analysis of non-reduced and unboiled unlabeled Fc (lane 1) and Au-Fc (lane 2). The majority of Fc protein migrated at a higher apparent molecular weight in the Au-Fc sample, demonstrating covalent attachment of 1.4 nm Nanogold. (d) Confocal

images (~5 μm below the apical surface) of FcRn-expressing MDCK cells after Au-Fc uptake (bar = 10 μm). Filter-grown monolayers were incubated with ~1 μM Au-Fc for one hour at pH 6 and processed for immunofluorescence using antibodies against FcRn (green; left panel) and Fc (red; middle panel) as described in the Supplementary Methods. The merged image (right panel) shows regions of colocalization as yellow. The nearly equimolar ratio of gold to protein in our Au-Fc samples (see Methods) suggested that most or all of the Fc detected by immunofluorescence contained gold. Untransfected MDCK cells showed only background levels of fluorescence when subjected to the same incubation and staining protocols (data not shown).

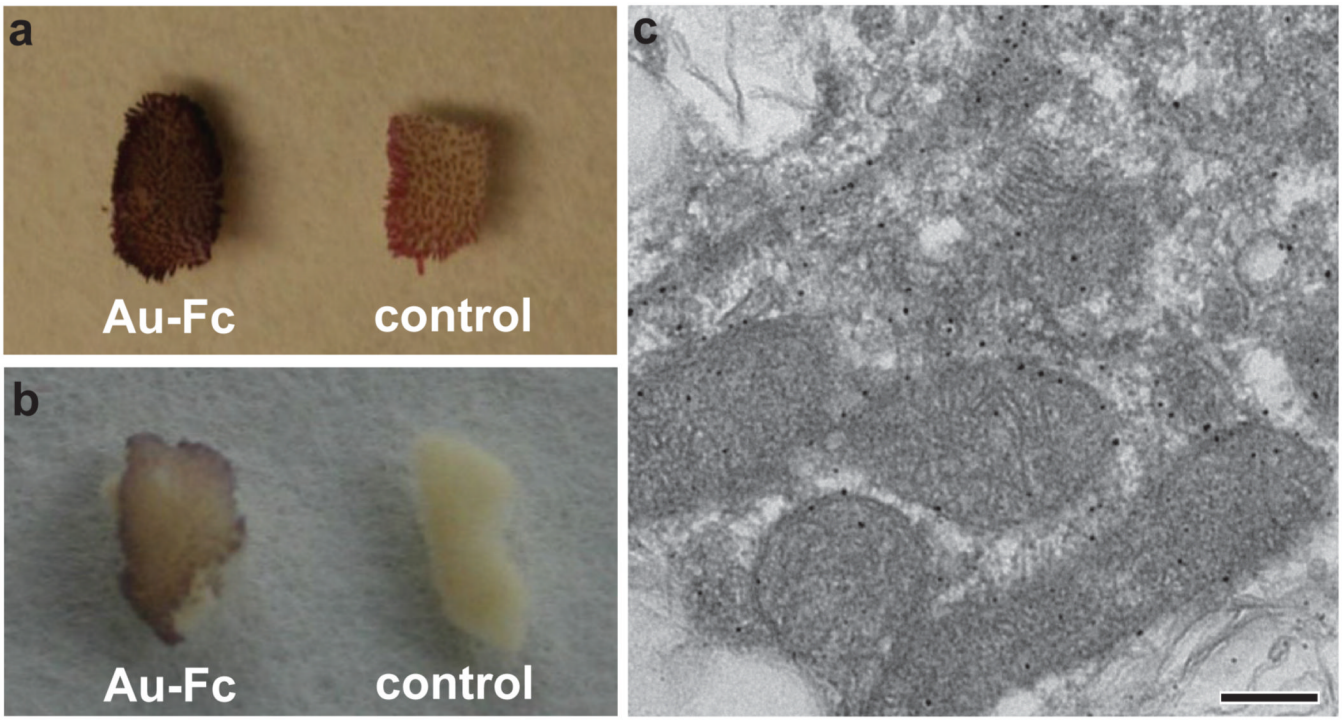

Figure 2.

Gold-enhanced, chemically-fixed intestinal segments. 13-day-old neonatal rats were fed ~2 μM Au-Fc or a control solution not containing Au-Fc prior to extraction, fixation and gold enhancement of duodenal samples. (a) Gold enhancement using GoldEnhance-EM 2113 (Nanoprobes, Inc.) following the manufacturer's protocol. (b) Gold enhancement using a modified protocol (Methods). The control sample derived using the modified protocol showed a significant decrease of background color development, which resulted from auto-nucleation, compared with the control sample prepared using the original protocol. (c) Projection EM image derived from a 120 nm section of the control sample shown in Panel a (bar = 200 nm). Randomly-distributed 5-10 nm background gold particles were found in mitochondria and regions of the cell that did not engage in FcRn-mediated endocytosis.

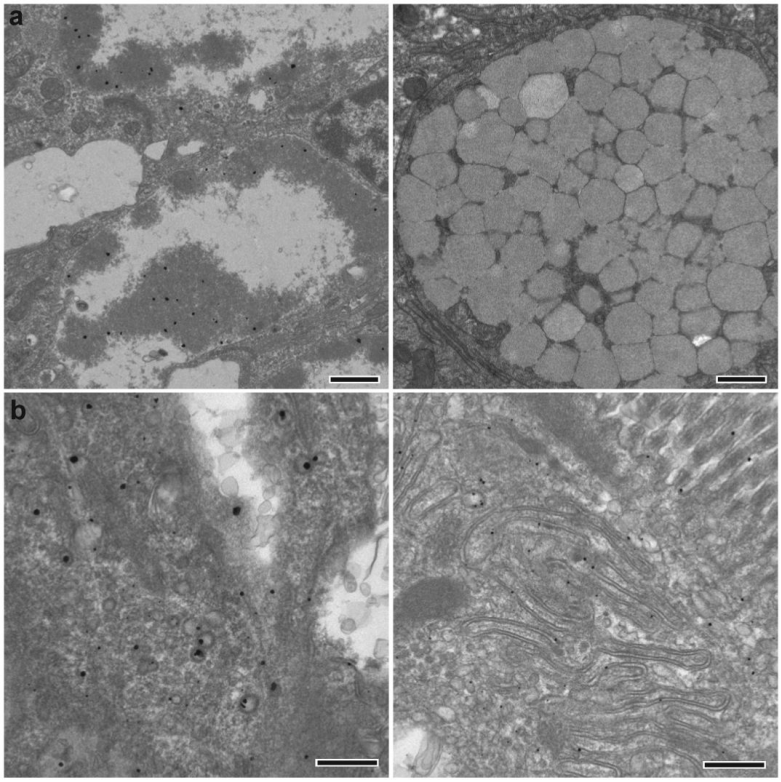

Figure 3.

Chemically-fixed, gold-enhanced samples of intestinal segments prepared using the modified enhancing protocol. (a) Specificity of gold enhancement in 70 nm sections derived from the distal small intestine (bar = 1000 nm). A region of the ileum (left) showed enhanced gold particles in giant lysosomes, consistent with fluid phase uptake of Au-Fc. By contrast, gold particles were not found in secretion vesicles in an adjacent goblet cell (right), demonstrating a lack of background resulting from auto-nucleation events. (b) Specificity of Au-Fc uptake and gold enhancement in sections derived from the proximal small intestine (bar = 500 nm). The section on the right was derived from the enhanced segment shown in Figure 2b. Gold particles were located in coated vesicles near the basolateral region of the cell (left; section thickness = 200 nm), on the surface of microvilli, in coated vesicles, and in the extracellular space near the apical surface of a cell (right; section thickness = 150 nm). The section on the left was gold enhanced in the absence of added gum arabic, resulting in specific enhancement of 1.4 nm Au-Fc, but a non-uniform particle size. The addition of gum arabic to the section on the right resulted in a more uniform (~20 nm) size of enhanced gold particle.

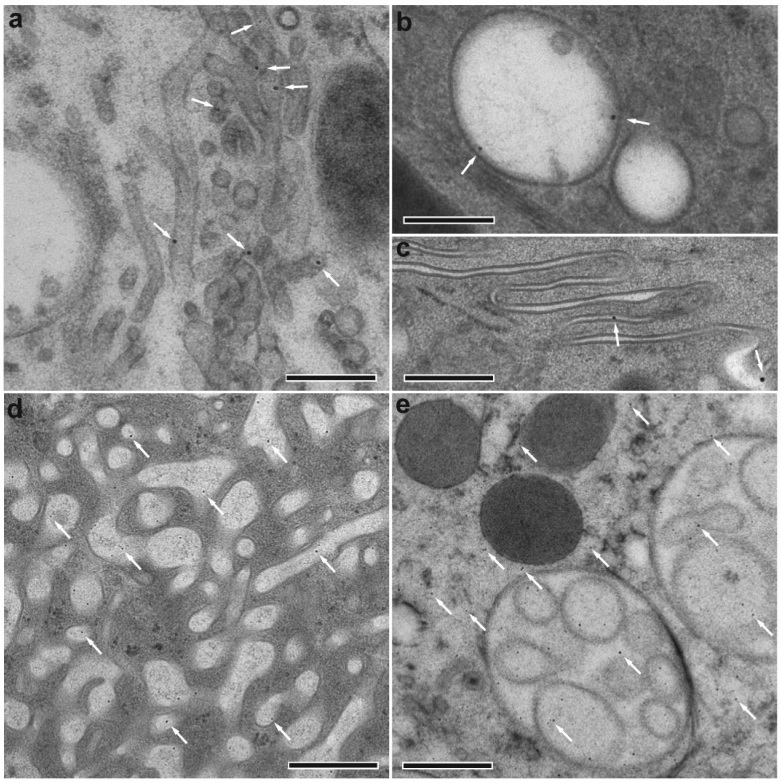

Figure 4.

Projection images of HPF/FSF samples of intestinal samples after silver enhancement/gold-toning/gold enhancement of 1.4 nm Au-Fc. (a) 150 nm section from the neonatal jejunum showing gold particles attached to inner surfaces of tubular vesicles, consistent with Au-Fc bound to FcRn (bar = 300 nm). (b) 150 nm section from the neonatal duodenum showing gold particles attached to the inner surface of a multivesicular body (bar = 300 nm). (c) 70 nm section from the neonatal duodenum showing gold particles after release into the extracellular space from the basolateral membrane (bar = 500 nm). (d) 120 nm section from the neonatal ileum showing enlarged gold particles distributed only inside apical vesicles (bar = 500 nm). (e) 120 nm section from the neonatal jejunum showing auto-nucleation resulting in small (~5 nm) background gold particles distributed randomly inside and outside of vesicles (bar = 500 nm). Auto-nucleation in this case might have resulted from over-exposure to $NaBH_4$ and/or too long of a developing time.

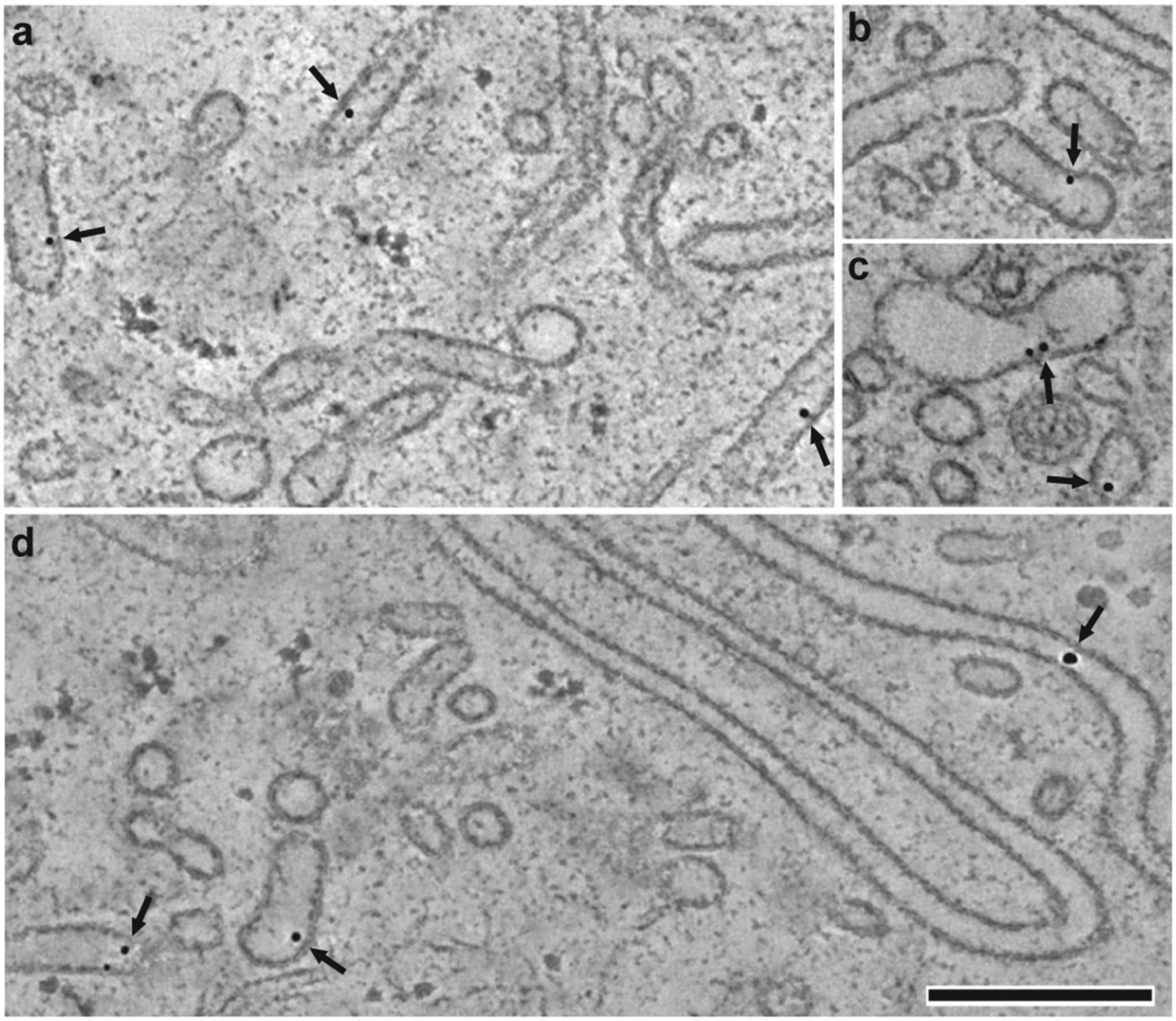

Figure 5.
Digital slices (1.6 nm) derived from tomograms of HPF/FSF samples of jejunal samples after silver enhancement/gold-toning/gold enhancement of 1.4 nm Au-Fc (bar = 300 nm). Dual axis tilt series were recorded at 6500x from 180nm sections at 120 kV on a Tecnai T12 microscope. Panels a-d show enhanced gold particles near the membranes of tubular and spherical vesicles. Panel d shows enhanced Au-Fc that was released into the lateral intercellular space between adjacent intestinal cells.